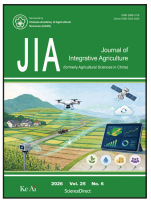
Journal of Integrative Agriculture 2026, 25(6): 2374–2388

Available online at ScienceDirect

Journal of Integrative Agriculture



RESEARCH ARTICLE

Quantifying the effects of nitrogen and potassium interactions on wheat using a new development index

Luchen Zhang, Longqin Wang, Yongchao Tian, Liang Tang, Bing Liu, Yan Zhu, Weixing Cao, Liujun Xiao, Leilei Liu#

National Engineering and Technology Center for Information Agriculture/Engineering Research Center of Smart Agriculture, Ministry of Education/Key Laboratory for Crop System Analysis and Decision Making, Ministry of Agriculture and Rural Affairs/Jiangsu Key Laboratory for Information Agriculture/Jiangsu Collaborative Innovation Center for Modern Crop Production, Nanjing Agricultural University, Nanjing 210095, China

Highlights

- Nitrogen (N)–potassium (K) interaction index (NKI) was constructed by combining critical N dilution curve (CNDC) and critical K dilution curve (CKDC).
- N status plays a more dominant role in N–K interactions during booting stage.
- NKI performed better than N nutrition index (NNI) and K nutrition index (KNI) for predicting yield under N–K interactions.

Abstract

Nitrogen (N) and potassium (K) are key elements for crop growth, yet studies on the impact of N–K interactions on plant N and K status and yield are lacking. This study aimed to develop effective indicators for diagnosing N and K nutrition and predicting the yield of wheat under N–K interactions based on the theoretical framework of a critical nutrient dilution curve. A 4-year N–K interaction experiment involving three wheat cultivars was employed for building and validating nutrient indices (NIs) based on the critical N dilution curve (CNDC) and the critical K dilution curve (CKDC). In addition, relevant data from the literature were collected for supplementary validation. The results revealed that changes in parameter A1 of the critical K dilution curves (CKDCs) can reflect the impact of nitrogen application on K absorption and utilization. However, the difference in K nutrition index (KNI) values calculated by CKDC under different N levels was not significant. Based on the aboveground biomass (AGB), a universal CKDC was established and defined as $K_c=3.63AGB^{-0.37}$ under N–K interactions. The results showed that the direct effects of N or K deficiency on crops could be quantified by the N–K interaction index (NKI) calculated by integrating CNDC and CKDC, and the changes in crop growth in response to proportional N and K concentrations could be determined by NKI as well. In addition, topdressing N fertilizer at the jointing stage significantly improved the N–K interaction effect on the N nutrition index (NNI) and NKI at the booting stage ($P<0.05$), but it had no significant N–K interaction effect on the KNI. All indicators at the heading stage demonstrated the best predictive capability for relative yield (RY) compared to other stages. Compared with NNI and KNI, the prediction accuracy of yield with NKI improved by 11.63 and 17.44%, respectively. The NKI has better performance in diagnosing N and K nutrition and predicting yield under N–K interactions than either NNI or KNI. This result enhances our understanding of the effects of N–K interactions on wheat growth and has important applications for improving the accuracy of N and K nutrition diagnosis and yield prediction.

Keywords: critical dilution curve, N–K interaction index (NKI), nutrition diagnosis, wheat, yield

1. Introduction

Nitrogen (N) and potassium (K) are essential macronutrients for plants and the two main factors limiting crop productivity (He *et al.* 2015; Yan *et al.* 2020). There is also a synergistic effect between N and K (Sattari *et al.* 2014; Adiele *et al.* 2022; Li *et al.* 2023), and the responsiveness of wheat yield to K uptake is influenced by N availability (Zhang *et al.* 2010). Improper application of N and K fertilizers can reduce

Received 11 September 2024; Received in revised form 19 December 2024; Accepted 20 December 2024; Available online 20 February 2025
#Correspondence Leilei Liu, E-mail: liuleilei@njau.edu.cn

© 2026 CAAS. Publishing services by Elsevier B.V. on behalf of KeAi Communications Co. Ltd. This is an open access article under the CC BY-NC-ND license (http://creativecommons.org/licenses/by-nc-nd/4.0/). Peer review under responsibility of Editorial Board of *Journal of Integrative Agriculture*.
doi: 10.1016/j.jia.2025.02.036

nutrient use efficiency, while balanced N and K management can prevent N losses, thereby mitigating the environmental impacts of excessive N application (Lollato *et al.* 2019; Grzebisz *et al.* 2020; Soratto *et al.* 2022). Therefore, the interactions and co-limitations between N and K must be considered (Sadras 2005) for assessing the N and K nutritional status of plants during the growing season, thereby optimizing fertilizer applications and increasing yields.

Compared to other nutrient diagnostic methods, such as critical nutrient concentrations (Bates 1971), the diagnosis and recommendation integrated system (DRIS) (Beaufils and Sumner 1976), the central method (Parent and Dafir 1992), and boundary lines (Vizcayno-Soto and Côté 2004), the critical N dilution curve (CNDC) has the advantage of considering the decline in plant nutrient concentration during the plant growth process (Williams 1957). Therefore, CNDC is extensively employed as a diagnostic tool for N adequacy and in simulations that predict crop yields (Lemaire 2012; Gómez *et al.* 2019; Soratto *et al.* 2022). Furthermore, the concept of CNDC was later extended to K (Lemaire *et al.* 2019), although there are few studies on the critical K dilution curve (CKDC) of wheat. Only Fontana *et al.* (2022) studied CKDC, but they just focused on the K nutrient while ignoring N–K interaction. Previous studies have found a positive N–K interaction in long term experiments (Zhang *et al.* 2010). The response of wheat to K increases with the N application rate, suggesting that more K fertilizer is needed when N rates are increased (Mondal 1982; Zhang *et al.* 2010). However, some studies have also reported that the concentration of K in plants remains relatively constant regardless of N supply. For example, K concentrations in ryegrass, measured in both dry matter and tissue water, consistently remained within a narrow range and were unaffected by treatment or time variations (Jarvis *et al.* 1990). The N application rate had minimal influence on the K concentrations in mature grains (Alfoldi *et al.* 1994). Therefore, the CKDC constructed by Fontana *et al.* (2022) cannot be used to diagnose N–K interaction conditions. It is necessary to further explore the impact of N application on the CKDC.

Based on the concepts of CNDC and CKDC, the N nutrition index (NNI) and K nutrition index (KNI) can be calculated to accurately evaluate the plant N and K nutritional status (Lemaire *et al.* 2019; Adiele *et al.* 2021). In some circumstances, NNI and KNI can be regarded as essential covariates for interpreting field data, particularly when emphasizing comparisons of genotypes and practices (Lemaire *et al.* 2019). Although using a single nutrient index can achieve the effect of nutrient diagnosis, this approach only addresses the deficiency of a single element and lacks any explanation for the N–K interaction effects. A suitable nitrogen-to-potassium concentration (N-to-K_c) ratio can maintain a relatively elevated photosynthetic capacity and plant biomass. Therefore, the ratio between N and K concentrations seems to be a general indicator for elucidating variations in the N and K concentrations across K supply and N conditions (Hou *et al.* 2018; Xie *et al.* 2020). In addition, Greenwood *et al.* (2008) observed a decline in the N:P ratio of aboveground biomass (AGB) across various annual crops during growth, which they attributed to changes in the proportions of growth-related and storage/structure-related tissues, and concluded that the N:P ratio is a function of crop biomass as was confirmed in the study of Bélanger *et al.* (2017).

Currently, the relationship of the N-to-K_c ratio to AGB remains unexplored in wheat. Investigating the diagnostic potential of the N-to-K_c ratio and integrating CNDC and CKDC for the concurrent diagnosis of multiple elements and yield prediction is imperative. Therefore, the objectives of this study were to: (1) establish a universal CKDC and combine it with CNDC to construct NKI under N–K interactions; (2) evaluate the impact of N–K interactions on plant N and K nutritional status; and (3) compare the performance of NKI with those of NNI and KNI in predicting wheat yield.

2. Materials and methods

2.1. Data sources

Multi-year fixed-point experiment Field trials were conducted at Rugao City, Jiangsu Province, China (32°38′N, 120°56′E) in the 2018–2019, 2019–2020, 2020–2021, and 2021–2022 growing seasons. The climate at the field site is described as semi-tropical monsoon and humid, with an average annual temperature of 15°C and precipitation of 1,055.5 mm. The tested soil has a loamy texture, with a pH of 7.78, organic matter of 20.6 g kg^{-1}, nitrate nitrogen of 6.8 mg kg^{-1}, ammonium nitrogen of 3.1 mg kg^{-1}, available K of 50.8 mg kg^{-1}, slowly available K of 390.8 mg kg^{-1} and total K of 10.9 mg kg^{-1} in the 20 cm topsoil.

A sequential block field trial consisting of three replicates with different levels of N and K fertilizers was conducted over a four-year period. Two N application rates (N1 and N2 at 120 and 240 kg ha^{-1} N, respectively) and three K application rates (CK, K150, and K300 at 0, 150 and 300 kg ha^{-1} K_2O, respectively) were used in the 2019 and 2020 wheat growing seasons. The same N application rates and another four K application rates (CK, K100, K200, and K300 at 0, 100, 200, and 300 kg ha^{-1} K_2O, respectively) were used in the 2021 and 2022 wheat growing seasons. The details of the treatments from 2019 to 2022 are summarized in Table 1. Urea (46% N) and potassium sulfate (83% K_2O) were used as the sources of N and K fertilizers, respectively. The N and K fertilizers were divided into basal fertilizer at the sowing stage and top dressing at the jointing stage with a ratio of 1:1. The basal fertilizer applied every growing season was superphosphate (12% P_2O_5), at a rate of 135 kg ha^{-1} P_2O_5. Fertilizers were spread evenly across each plot (4.5 m×6 m) and mixed thoroughly using a rake to ensure proper distribution.

The cultivars tested in the three growing seasons from 2019 to 2021 were Shengxuan 6 (SX06, medium gluten wheat, bred and released by Jiangsu Academy of Agricultural Sciences, Nanjing, China in 2009) and Yangmai 22 (YM22, weak gluten wheat, bred and released by the Agricultural Research Institute of Lixiahe Region, Yangzhou, China in 2012). In the 2022 growing season, the cultivars were SX06 and Yangmai 23 (YM23, strong gluten wheat, bred and released by Jiangsu Kingearth Seed Co., Ltd., Yangzhou, China in 2013). Wheat was planted at the end of October in each year, with a row spacing of 30 cm and a seeding

Table 1 Details of fertilizer treatments in the field

Years	Cultivar[1)]	N treatment	K treatment	N rate (kg ha^{-1} N)	K rate (kg ha^{-1} K_2O)
2018–2020	SX06 YM22	N1	CK	120	0
			K150	120	150
			K300	120	300
		N2	CK	240	0
			K150	240	150
			K300	240	300
2020–2022	SX06 (2020–2022) YM22 (2020–2021) YM23 (2021–2022)	N1	CK	120	0
			K100	120	100
			K200	120	200
			K300	120	300
		N2	CK	240	0
			K100	240	100
			K200	240	200
			K300	240	300

[1)] SX06, YM22 and YM23 represent Shengxuan 6, Yangmai 22 and Yangmai 23, respectively.

rate of 300 kg ha^{-1}, and it was harvested at the end of May of the following year. Other field management protocols to control pests and diseases adhered to local standards.

Sampling and measurements Destructive sampling was performed at the key growth stages of wheat, from tillering to maturity. Plant samples collected at each stage were meticulously divided into their corresponding components, including leaves, stems, ears, and grains. The samples were incubated at 105°C for 30 min to inactivate enzymes and other proteins. The samples were subsequently dried to a constant weight at 80°C, after which the biomass of each organ was weighed. Dried samples were ground to measure the N and K concentrations. In this study, the N concentration was analyzed according to the Dumas combustion method with an elemental analyzer (vario MACRO cube; Elementar, Hanau, Germany). A portion of the powder was digested with H_2SO_4 and H_2O_2 until the solution became transparent, after which the samples were diluted, and the K concentration was determined with an ICE3000 AAS (Thermo Fisher, Inc., Sunnyvale, CA, USA). The concentration of plant N (PNC) (g kg^{-1}) was calculated according to Huang *et al.* (2018). The method for calculating the plant K concentration (PKC) (g kg^{-1}) mirrored that of PNC.

Data collection In addition to the field experiment data above, data from the literature were also collected to validate the applicability of the newly developed index NKI for diagnosing N and K nutrients and predicting yield under different N–K interaction conditions. This survey combined information from N and K interaction experiments on wheat published between 2004 and 2020 and obtained through Google Scholar (http://scholar.google.com/) and the China National Knowledge Infrastructure database (http://www.cnki.net/). The search keywords used included 'nitrogen and potassium interaction', 'nitrogen and potassium combined fertilization', 'wheat', 'dry matter' and 'yield'. A validation analysis was used to filter the identified studies to only those that satisfied the following specific criteria: (i) the field experiments included one or more K fertilizer application rates and at least one N fertilizer application rate, and (ii) the experiments must also provide the nitrogen and potassium concentrations in plants, the aboveground biomass of at least three vegetative growth stages, and final yield. A total of 1,090 papers were identified based on the titles, 1,014 of which were eliminated based on their keywords and abstracts. Ultimately, after checking the availability of data in the remaining literature, 10 experiments in the four wheat production provinces that met the inclusion criteria and had the required data types were selected. The details of site information and management practices for each experiment (including the above-mentioned multi-year fixed-point experiment) are listed in Table 2.

2.2. Data analysis

This study is divided into three steps. First, the multi-year fixed-point nitrogen–potassium interaction experiments and literature searches were conducted to obtain the corresponding data. Then, based on two years of field data, a Bayesian approach was used to construct the CKDC, and KNI and NNI were further constructed based on the CKDC and CNDC, respectively. Then, NKI was constructed by integrating the CKDC and CNDC. Finally, the independent field trial data and literature data were used to assess the effectiveness of the new index for nutritional diagnosis and yield prediction (Fig. 1).

Construction of critical K concentration dilution curves The Bayesian Statistical Model (Makowski *et al.* 2020) was employed to fit the CKDC of wheat in this study. This approach assumes that the response of AGB to PKC follows a linear+plateau function. The probability distribution estimated through the Bayesian method characterizes the uncertainty surrounding parameters of the linear+plateau function on the observation date, and then the parameters of the CKDC are derived from the posterior probability distribution of the fitted model parameters. This method does not require distinguishing between K-limited data and non-K-limited data and can quantify the uncertainty of parameter estimates, thereby allowing comparisons of differences in the estimated CKDC models for different cultivars and N treatments. The CKDC based on AGB was calculated with eq. (1):

$$K_c = A1 \times AGB^{-A2} \quad (1)$$

where K_c is the critical K concentration value (%), AGB is the aboveground biomass (t ha^{-1}), A1 is the critical K concentration value when the aboveground biomass is 1 t ha^{-1}, and A2 is the dilution rate of the curve.

The Markov Chain Monte Carlo (MCMC) algorithm, based on the Bayesian Model, was employed to compute the posterior distributions of model parameters A1 and A2, and the algorithm was implemented using the R package rjags (Plummer 2017). This study fitted the AGB-based K_c dilution curves for different cultivars and N levels. In the fitting process, model 1 (Ciampitti *et al.* 2021) and weak prior information (prior 1) were used according to previously described methods, and the prior range of parameters was appropriately adjusted in some specific scenarios. The specific steps were as follows: the MCMC algorithm was first executed using three chains, with each chain comprising 50,000 iterations. Following a convergence check, an

Table 2 Summary of the experiments from the field and literature survey

Experiment	Site[1)]	Year	Cultivar[2)]	Sowing date	N rates (kg ha^{-1})	K rates (kg ha^{-1})
1	Feidong (117°47′E, 31°88′N)	2004–2005	WM48	10.15	0–150–180–210	0–75–150
2	Mengcheng (116°15′E, 32°55′N)	2004–2005	YN19	11.06	0–120–180	0–90–150
3	Qingyuan (113°40′E, 38°10′N)	2010–2011	JM22	10.08	195–255–270–300	75–120–150
4	Qingyuan (113°40′E, 38°10′N)	2010–2011	JM22	10.08	255	0–48–84–120–156
5	Tai'an (116°54′E, 36°12′N)	2018–2019	GY5766 TM198	10.03	144–192–240	120
6	Tai'an (116°54′E, 36°12′N)	2019–2020	GY5766 TM198	10.03	144–192–240	120
7	Rugao (120°33′E, 32°23′N)	2018–2019	SX06 YM22	10.28	120–240	0–150–300
8	Rugao (120°33′E, 32°23′N)	2019–2020	SX06 YM22	10.28	120–240	0–150–300
9	Rugao (120°33′E, 32°23′N)	2020–2021	SX06 YM22	10.27	120–240	0–100–200–300
10	Rugao (120°33′E, 32°23′N)	2021–2022	SX06 YM23	10.30	120–240	0–100–200–300

[1)] Feidong and Mengcheng, Anhui Province; Qingyuan, Hebei Province; Tai'an, Shandong Province; Rugao, Jiangsu Province, China.
[2)] WM48, YN19, JM22, GY5766, TM198, SX06, YM22, and YM23 represent Wanmai 48, Yannong 19, Jimai 22, Gaoyou 5766, Taimai 198, Shengxuan 6, Yangmai 22, and Yangmai 23, respectively.

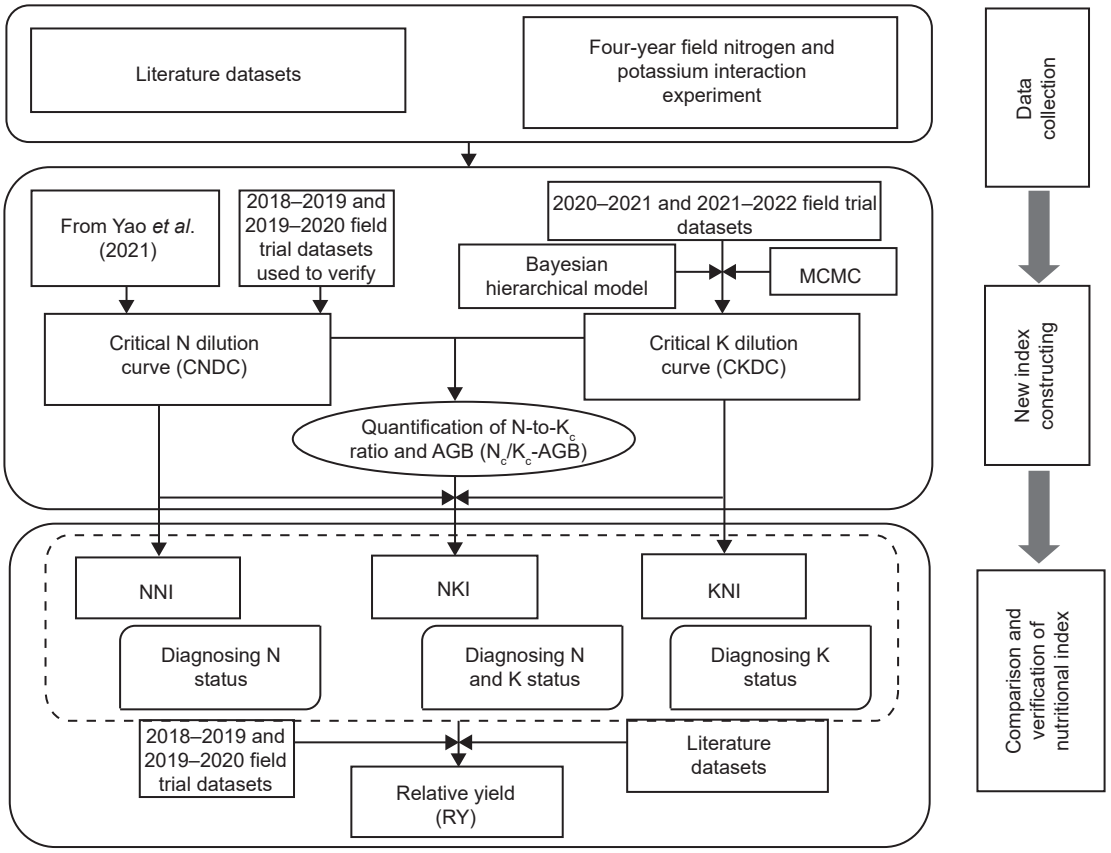


Fig. 1 Workflow for the development of a new index to diagnose N and K status and predict yield under N–K interactions. N-to-K_c ratio, nitrogen to potassium concentration ratio; AGB, aboveground biomass; NNI, nitrogen nutrition index; KNI, potassium nutrition index; NKI, nitrogen-potassium interaction index; MCMC, Markov Chain Monte Carlo.

additional 100,000 iterations were performed. Then the obtained parameter value samples were used to calculate the median and 95% confidence interval (CI) of each parameter of the K_c dilution curve under different N levels for each cultivar, thereby obtaining the K_c dilution curve model under every specific scenario. The universal K_c dilution curve combines, runs and converges all scenario data points to calculate the 95% CI and median for parameters A1 and A2.

To determine the status of K in the plant, the KNI values of the different cultivars were further calculated for each sampling date, which were calculated as follows:

$$KNI=\frac{K_a}{K_c} \quad (2)$$

where K_a is the actual K concentration (%) of the plants observed in each growth period, calculated using the K_c curve equation obtained by the Bayesian method. KNI=1 indicates that the K nutritional status is optimal, while KNI>1 and KNI<1 indicate K excess and deficiency, respectively.

N status of plants under N–K interactions The traditional critical N concentration (N_c) dilution curve based on AGB is shown in eq. (3) (Justes *et al.* 1994):

$$N_c=a\times AGB^{-b} \quad (3)$$

where AGB is the aboveground biomass (t ha^{-1}), *a* is the critical N concentration value when the aboveground biomass is 1 t ha^{-1}, and *b* is the dilution rate of the curve. Here, the values of *a* and *b* are consistent with Yao *et al.* (2021), i.e., *a*=3.90 and *b*=0.41.

NNI was further calculated with the ratio of N_a and N_c to quantify the impact of N and K on crop N status (Lemaire *et al.* 2008):

$$NNI=\frac{N_a}{N_c} \quad (4)$$

where N_a is the actual N concentration (%) of the plant during each growth period. NNI=1 indicates that the N nutritional status is optimal, while NNI>1 and NNI<1 indicate N excess and deficiency, respectively.

Construction of the NKI Although NNI and KNI can be used to diagnose N and K deficiencies in plants, respectively, they cannot adequately capture the nutrient deficiency status that arises from N and K interactions. To comprehensively evaluate the impact of N–K interactions on plant nutrient status, this study constructed a comprehensive index, NKI, that can simultaneously characterize N and K deficiency. The calculation formula is:

$$NKI=\frac{N_a/K_a}{N_c/K_c} \quad (5)$$

where N_a/K_a and N_c/K_c represent the actual nitrogen–potassium ratio (%) and critical nitrogen–potassium ratio (%), respectively. Here, NKI<1 indicates that the proportion of N deficiency is greater than the K deficiency; NKI=1 indicates that N and K nutrition are reduced in similar proportions; and NKI>1 indicates that N has accumulated in excess based on the K nutritional content of the wheat. In this way, the deficiencies of N and K nutrients under N–K interactions can be analyzed simultaneously.

Assessment of NKI To evaluate the effect of NKI on crop N and K nutrition under N–K interactions, the ratio between the crop accumulative nitrogen and potassium ratio deficit (N/K_{ad}) can be calculated. Here, N/K_{ad}=0, <0 and >0 indicate an appropriate nitrogen-potassium ratio, a nitrogen-potassium ratio surplus and a nitrogen-potassium ratio deficit, respectively. The specific calculation is:

$$N/K_{ad}=\left(\frac{N_c}{K_c}-\frac{N_a}{K_a}\right)\times AGB \quad (6)$$

By analyzing the correlation between the NKI and N/K_{ad}, the effect of NKI on crop N and K nutrition under N–K interactions can be evaluated.

In addition, this study verified and evaluated the ability of NKI to predict crop yield under N–K interactions by comparing and quantifying the correlations between NNI, KNI and NKI and the relative yield (RY). RY was calculated by dividing the yield of each treatment by the maximum yield treatment (Ziadi *et al.* 2008):

$$RY=\frac{Y}{Y_{max}} \quad (7)$$

where Y and Y_{max} represent the measured yield of each treatment (t ha^{-1}) and the maximum value of the measured yield (t ha^{-1}), respectively.

2.3. Statistical analysis

The statistical analysis of relevant indicators was performed using SPSS 25.0 software (SPSS, Inc., Chicago, USA). The comparison of average values between different treatments was performed using the least significant difference (LSD) method for analysis of variance (P<0.05) of nitrogen fertilization, potassium fertilization and their interaction. All the results were visualized using Origin 2023 software (Origin Lab, Massachusetts, USA).

3. Results

3.1. Construction and valuation of K_c dilution curves

The field experiment data from the 2020–2021 and 2021–2022 seasons were used to construct the CKDCs. Fig. 2 illustrates the CKDCs based on AGB for different cultivars and N levels (nine scenarios), which revealed that PKC gradually decreased with increasing AGB in all scenarios, and the CKDC uncertainty level (width of 95% CI) decreased with increasing AGB. Regardless of the N application level and cultivar, the median CKDC fit was greater than the K_c value obtained for the CK (0 kg ha^{-1} K_2O). At the N1 level, the median CKDC fit was lower than the K_c value obtained at a K application rate of 200 kg ha^{-1}, closely approximating the K300 treatment.

Curve fitting was performed for the three scenarios for the N1-all cultivars, N2-all cultivars, and all N-all cultivars combinations, and the results were compared with the curves created for the nine scenarios (Fig. 3). Fig. 3 shows the post-median CKDC parameters under each scenario along with their corresponding 95% CIs, which cover 95% of the values sampled in the MCMC posterior distribution. When summarized by cultivar, the ranges of A1 and A2 for all cultivars at the N1 level were 2.90 (95% CI=(2.73, 3.07)) and 0.29 (95% CI=(0.26, 0.32)), respectively, and the ranges of A1 and A2 for all cultivars at the N2 level were 3.90 (95% CI=(3.63, 4.20)) and 0.35 (95% CI=(0.31, 0.38)), respectively. Furthermore, when fitting to the entire dataset (all N levels and all cultivars), the median values for parameters A1 and A2 were 3.63 and 0.37, respectively. Compared to the individual curves for each scenario, the confidence interval for the overall CKDC was reduced to 0.66% K (at 1 t ha^{-1}), while that for biomass (at 13 t ha^{-1}) was reduced to 0.07% K, illustrating greater uncertainty at lower AGB than at higher AGB.

For parameter A1, there were significant differences between the fitting curves of all cultivars under the N1 and N2 levels, but there was no difference between the global fitting curve parameters and those of the fitting curves for the N1 and N2 levels (Fig. 4-A). Compared with parameter

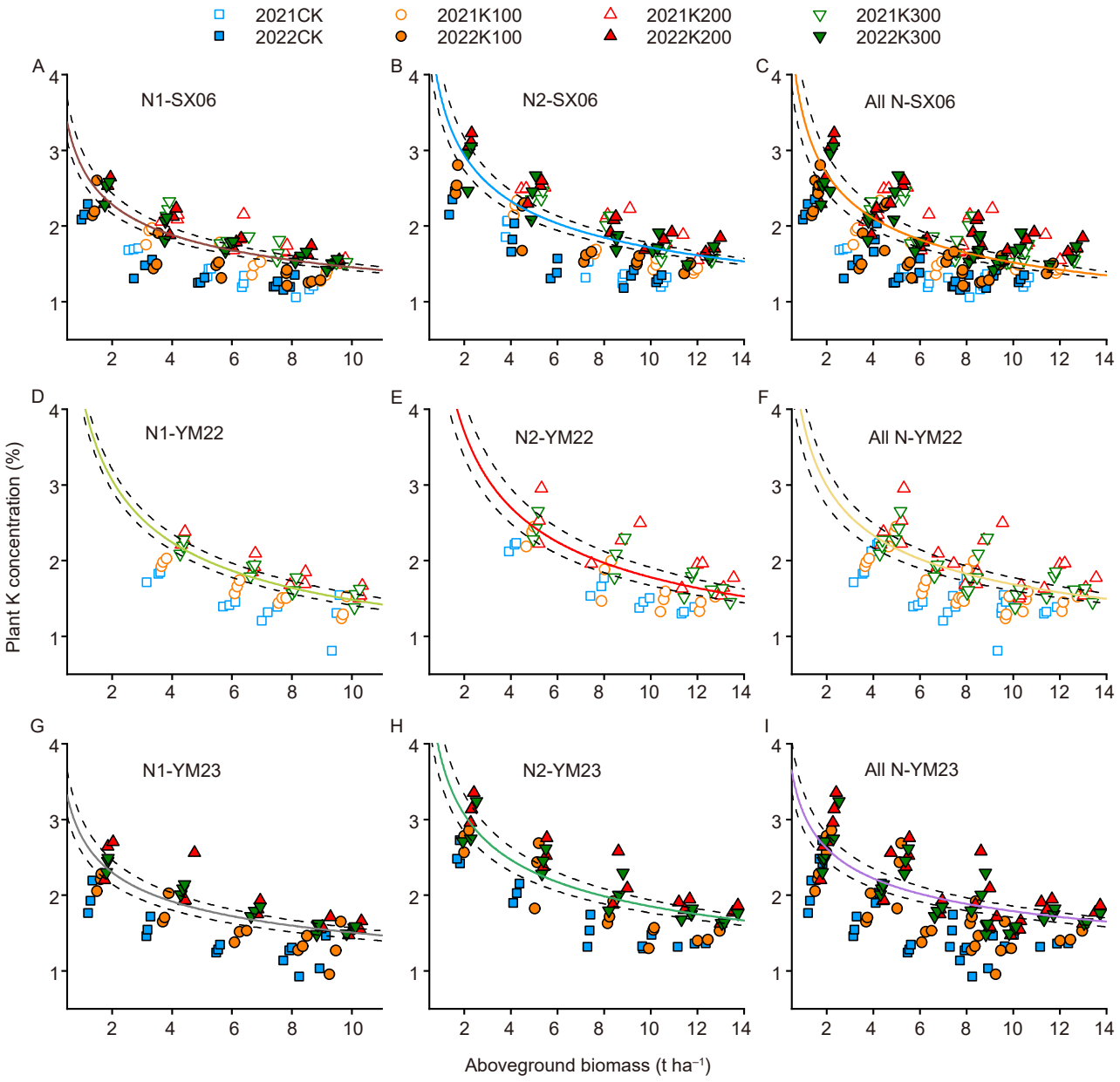


Fig. 2 Relationships between plant K concentration (PKC) and aboveground biomass (AGB) in nine scenarios combining three cultivars and two growing seasons. The solid and dotted lines represent the median and 95% confidence interval (CI) of critical K dilution curve (CKDC), respectively. SX06, YM22 and YM23 represent Shengxuan 6, Yangmai 22 and Yangmai 23, respectively. N1 and N2 indicate N application amounts of 120 and 240 kg ha^{-1} respectively. CK, K100, K200, and K300 indicate K application amounts of 0, 100, 200, and 300 kg ha^{-1}, respectively.

A1, the impact of different N levels on parameter A2 was not significant (P>0.05). Overall, the N–K interactions increased the variability of parameter A1 but had no significant impact on parameter A2 (Fig. 4-B). Except for a significant difference in the N2 level for YM22, the A1 curve parameters from the global fitting were not significantly different (P>0.05) from the fitting parameters in the other scenarios (Fig. 4).

There were significant differences among the KNI values for the nine scenarios. Nevertheless, these differences were relatively small, particularly among the individual cultivars under all N levels according to the global fit curve (Fig. 5). Compared to the KNI values calculated for each cultivar with a single N level, the RMSE values were lower after pooling all the N levels. The RMSE values for SX06, YM22 and YM23 were 0.04, 0.07, and 0.07, respectively (Fig. 5-C, F and I). These results indicate that when using the global fitting curve (for all N levels and all cultivars) for KNI calculations, the deviations between the KNI calculated by most specific scenario curves and the global curve are minimal, except for those calculated by the N2 level for both YM22 and YM23.

3.2. Effects of N–K interactions on the N and K nutritional status of wheat

N status of plants under N–K interactions The corresponding

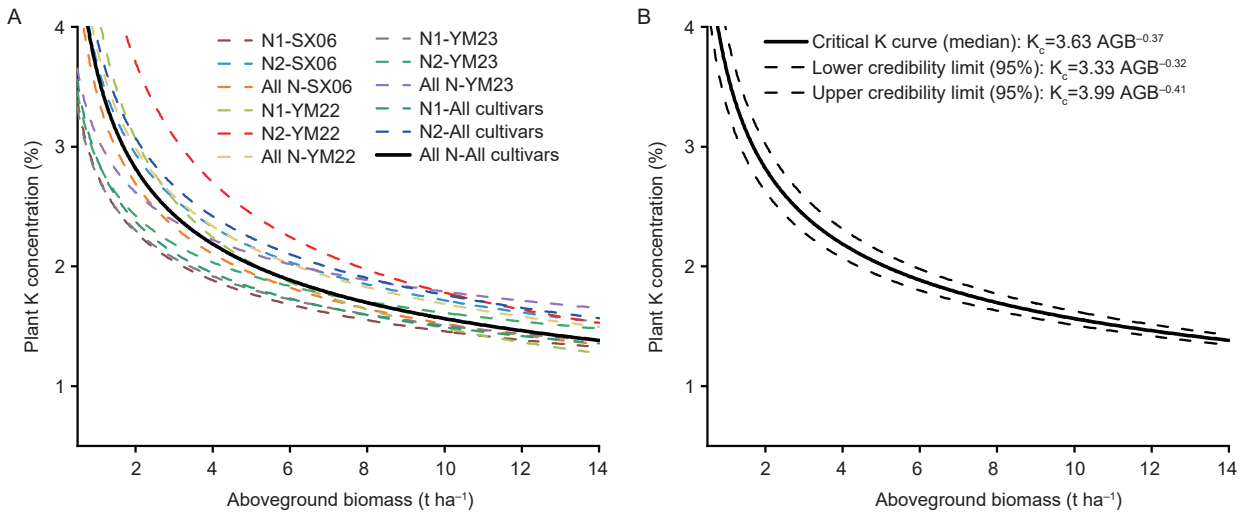


Fig. 3 Relationships between plant K concentration (PKC) and aboveground biomass (AGB) during the vegetative growth period, including the critical K dilution curve (CKDC) under a specific scenario and all other scenarios (A), and the 95% confidence intervals (CI)s for the upper and lower levels of the global fitted critical curve (B). The solid line represents the global CKDC of the Bayesian fit for all scenarios in the dataset, and the dashed line corresponds to the wheat CKDC observed for a specific scenario (A). N1 and N2, 120 and 240 kg ha^{-1}, respectively. SX06, Shengxuan 6; YM23, Yangmai 23. K_c, potassium concentration.

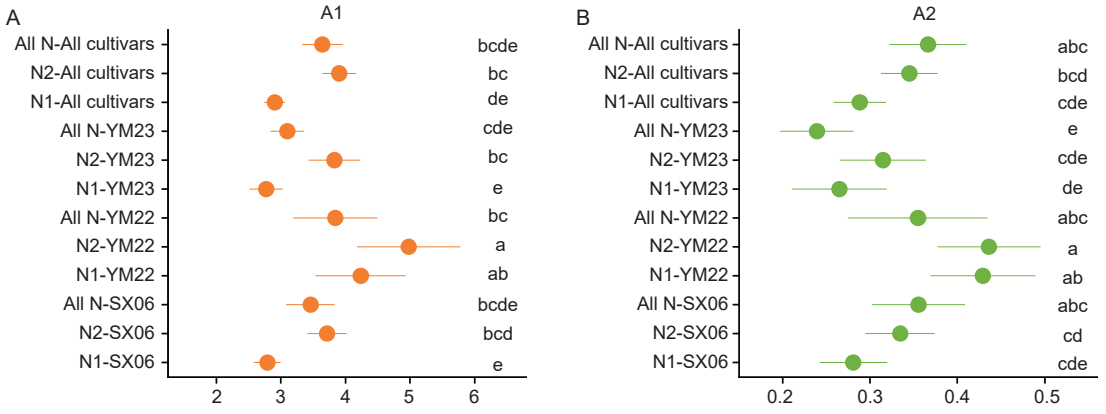


Fig. 4 Estimates of the posterior median and 95% confidence intervals (CIs) of parameters A1 and A2 obtained by Bayesian methods. N1 and N2, 120 and 240 kg ha^{-1}, respectively. SX06, Shengxuan 6; YM23, Yangmai 23. Different letters represent significant differences between the 95% CIs based on comparisons between different scenarios.

NNI was calculated using field trial data from the 2018–2019 and 2019–2020 seasons (Fig. 6). During the entire growth period before the flowering of wheat, the dynamics of NNI were similar among the different cultivars and under different N and K conditions. During the four growth stages, NNI increased significantly (P<0.05) with increasing N and K application rates. Under the N1 level, lower N rates resulted in NNI values less than 1 for all the K treatments in the early growth period. Moreover, under the N2 level for YM22, the values for the different K treatments exceeded 1 at all four growth stages, suggesting that adequate or even excess N had been applied. Compared to the control treatment CK, applying K at the jointing stage significantly (P<0.05) increased the NNI for the two cultivars at the booting stage but had no significant (P>0.05) effect on the NNI at the heading to flowering stage. Significant (P<0.05) effects of N–K interactions on the NNI of the two cultivars at the booting stage were observed in both growing seasons, with no significant (P>0.05) interaction effects found in the other growth stages.

Dynamic changes in the KNI under N–K interactions Like NNI above, the KNI of wheat plants was calculated based on the global CKDC constructed for different cultivars and N levels. The KNI of the different wheat cultivars exhibited a declining trend as the growth period progressed (Fig. 7). During each growth period, KNI increased with increasing K application. Under a given K level, the KNI value under the N2 level was greater than that under the N1 level, and no significant (P>0.05) N–K interactions were observed throughout the entire growth period of the two cultivars.

Dynamic changes in NKI under N–K interactions By using the CNDC and CKDC, the relationship between the

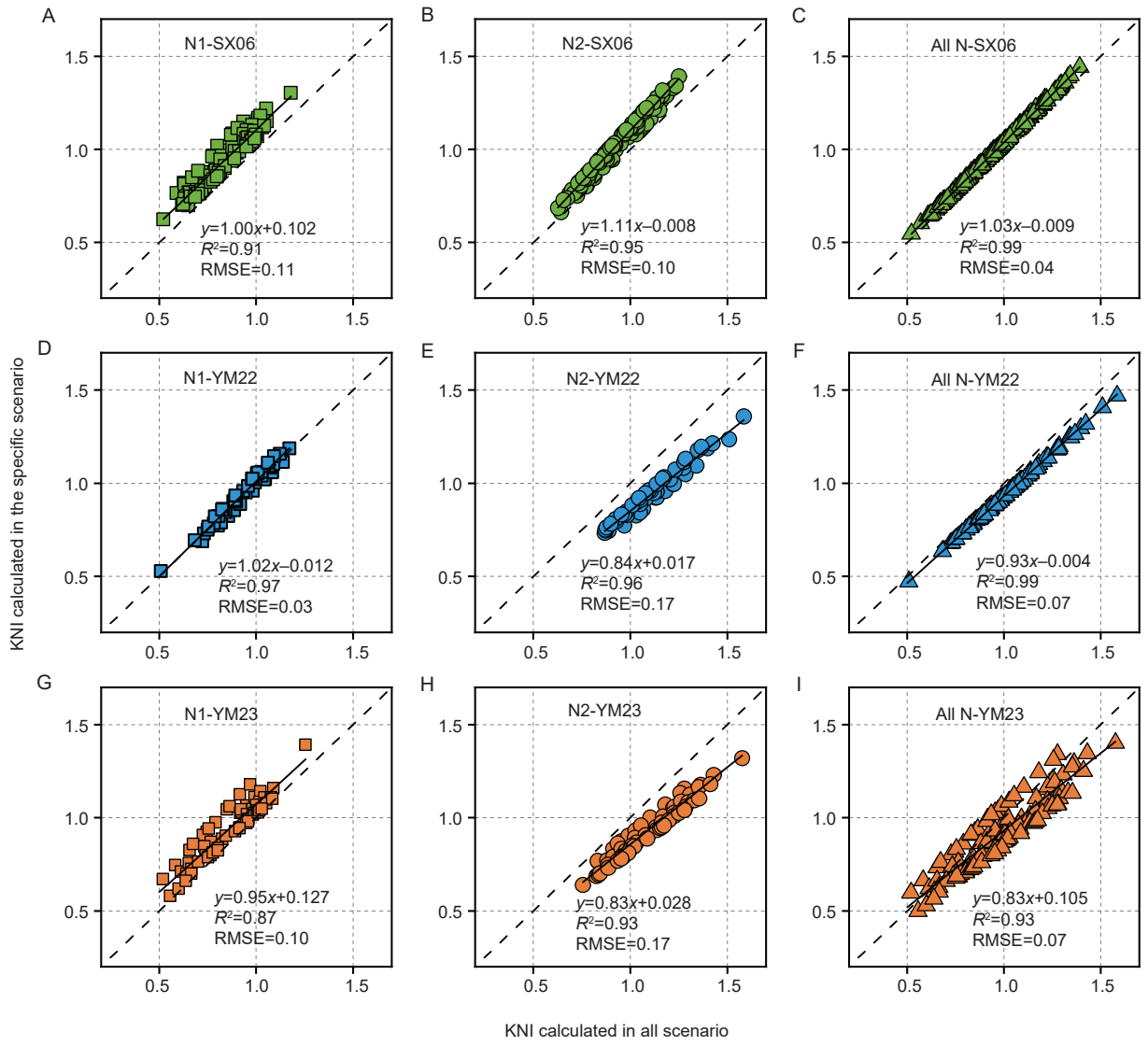


Fig. 5 Relationships between the K nutrition index (KNI) calculated from the Bayesian fitted critical K dilution curve (CKDC) data for a specific scenario and all the other scenarios. Different colors represent the three cultivars; ■ represents the cultivars at the N1 level (A, D, and G); ● represents the cultivars at the N2 level (B, E, and H); and ▲ represents the cultivars at all N levels (C, F, and I). N1 and N2, 120 and 240 kg ha^{-1}, respectively. SX06, Shengxuan 6; YM23, Yangmai 23.

nitrogen to potassium concentration (N-to-K_c) ratio and AGB was derived and represented by $N_c/K_c=1.07AGB^{-0.04}$. Subsequently, the NKI was calculated based on eq. (5). The dynamic changes in the NKI for the different cultivars and under the N and K conditions were similar to those in the NNI, in which NKI slowly increased as the growth period progressed (Fig. 8). Compared with the N1 treatment, the increase in K fertilizer application from the jointing stage to the booting stage in the N2 treatment significantly (P<0.05) reduced the NKI. The NKI value of SX06 under the N1 treatment was less than 1 throughout most of the growth period, while the NKI value of YM22 was lower than 1 except in the early growth period and gradually became greater than 1 as the growth period progressed. For the N1 treatment in both years, the NKI of SX06 ranged from 0.59 to 1.27, and the NKI of YM22 ranged from 0.77 to 1.35. For the N2 treatment, the NKI of SX06 ranged from 0.85 to 1.61, and the NKI of YM22 ranged from 0.93 to 1.67. N and K applications had significant interactive effects on the NKI at the booting stage in both cultivars (P<0.05) during the four growing seasons.

Dynamic changes in the accumulative nitrogen–potassium ratio deficit under N–K interactions To better determine the status of N and K under the common limitation of N and K, the effect of N–K interactions on plant N and K nutrition was quantified by calculating the accumulative nitrogen and potassium ratio deficit (N/K_{ad}). The N/K_{ad} ratio was calculated based on field trial data from the 2018–2019 and 2019–2020 seasons, and the results are illustrated in Fig. 9. Overall, across the different cultivars and N levels in both years, the N/K_{ad} ratio gradually decreased as the growth stage progressed. During each growth period, N/K_{ad} decreased with increasing N application and increased with increasing K application. Under a given K level, increasing

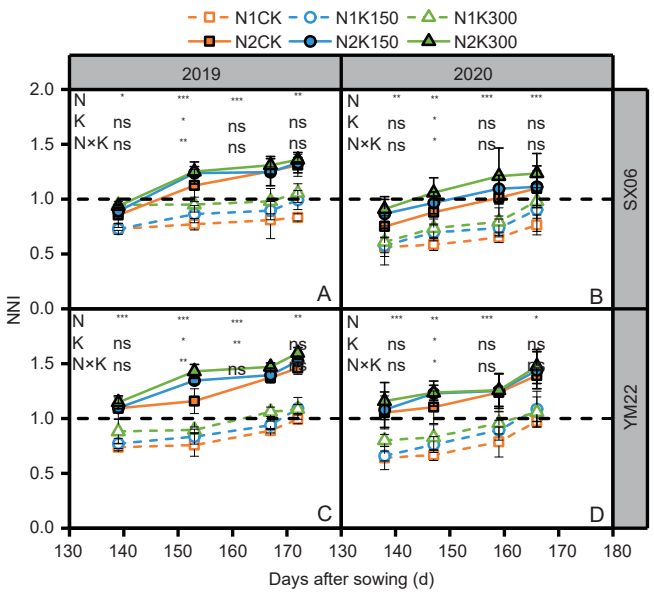


Fig. 6 Effects of N–K interactions on the N nutrition index (NNI) of different wheat cultivars during the growing seasons in 2018–2019 (A) and (C) and 2019–2020 (B) and (D). N, K and N×K refer to the effects of N fertilizer, K fertilizer and N–K interactions, respectively. SX06 and YM22 represent Shengxuan 6 and Yangmai 22, respectively. N1 and N2 represent N application rates of 120 and 240 kg ha^{-1}, respectively; and CK, K150 and K300 represent K application rates of 0, 150 and 300 kg ha^{-1}, respectively. Bars mean SD (n=3). *, ** and *** indicate significant differences at the 10, 5 and 1% levels, respectively; ns indicates no significant difference.

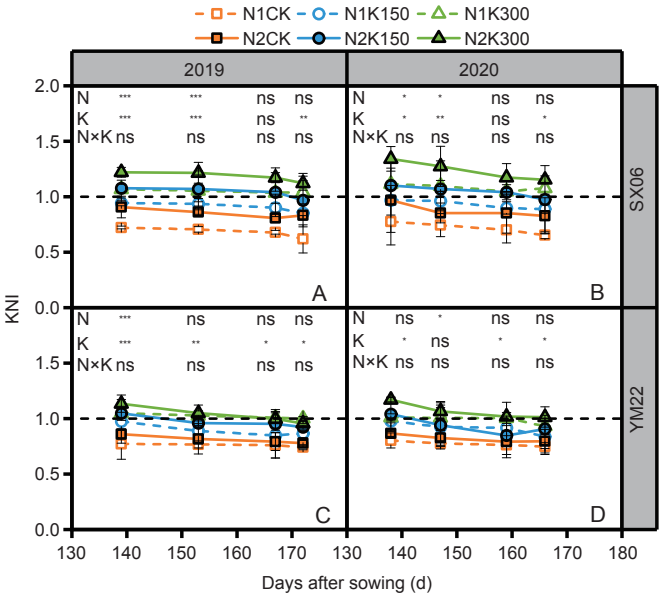


Fig. 7 Effects of N–K interactions on the K nutrition index (KNI) of different wheat cultivars during the growing seasons in 2018–2019 (A) and (C) and 2019–2020 (B) and (D). The results in this figure are verification results of field test data from the 2018–2019 and 2019–2020 seasons. SX06 and YM22 represent Shengxuan 6 and Yangmai 22, respectively. N1 and N2 represent N application rates of 120 and 240 kg ha^{-1}, respectively. CK, K150 and K300 represent K application rates of 0, 150 and 300 kg ha^{-1}, respectively. Bars mean SD (n=3). *, ** and *** indicate significant differences at the 10, 5 and 1% levels, respectively; ns indicates no significant difference.

the amount of N applied during the jointing–booting stage significantly (P<0.05) reduced N/K_{ad}. Under the N1 treatment in both years, the range of variation in the N/K_{ad} ratio of SX06 was –1.77 to 3.15 t ha^{-1}, whereas that of YM22 was –4.33 to 2.20 t ha^{-1}. Under the N2 treatment, the range of variation in the N/K_{ad} of SX06 was –6.36 to 1.31 t ha^{-1}, whereas that of YM22 was –7.24 to 0.51 t ha^{-1}. Compared with SX06, increasing N fertilizer application at the jointing stage in YM22 resulted in a more significant (P<0.05) reduction in N/K_{ad} between the treatments.

Relationship between NKI and N/K_{ad} To assess the applicability of the NKI constructed based on the critical nitrogen to potassium concentration ratio dilution curve based on AGB (N_c/K_c-AGB) for N and K management, field trial data from the 2018–2019 and 2019–2020 seasons in Rugao were used to analyze the quantitative relationship between NKI and N/K_{ad}. Irrespective of the cultivar or N level, the NKI of the wheat plants in the two years was significantly negatively correlated with N/K_{ad} (Fig. 10). Based on the R^2 of the fitting accuracy, when the two cultivars were considered together, the high N level resulted in greater values than the low N level. Overall, in the case of K application, the N/K_{ad} ratio in the N2 treatment was lower than that in the N1 level. There was no significant (P>0.05) difference in the relationship between the N/K_{ad} and NKI of the two cultivars at the same N level; i.e., under high N conditions, either with or without K application, most data points fell into the area characterizing excess cumulative N-to-K_c ratios. Compared with high-N conditions, most of the data points in the K fertilization treatment under low-N conditions were in the cumulative N-to-K_c ratio deficit area, and most of the CK treatment data points were in the cumulative N-to-K_c ratio surplus area. The distribution area of data points in the K150 treatment was greater in the N2 treatment than in the N1 treatment.

To further demonstrate the universality of the NKI constructed based on the N_c/K_c-AGB curve, additional verification was conducted using experimental data from four sites in the main winter wheat production provinces of China. The results indicated that the patterns of change in the relationships between NKI and N/K_{ad}, i.e., the optimal N and K management measures at each site calculated based on the N_c/K_c-AGB curve, were consistent with the verification data from Rugao (Fig. 11). There were no significant differences (P>0.05) in the fitting parameters between the sites at Mengcheng and Feidong in Anhui Province. Compared with those from Mengcheng, the data points from Feidong accounted for a larger proportion of the cumulative N-to-K_c ratio deficit area. Compared with those in Hebei and Anhui, the site of Tai'an in Shandong Province exhibited a greater difference in the proportion of the cumulative N-to-K_c ratio deficit and surplus. These results suggest that management measures at various sites can be further optimized based on the NKI, with particular emphasis on the Tai'an site.

3.3. Relationships between the nutritional indices and RY

Field experiment data from the 2018–2019 and 2019–2020

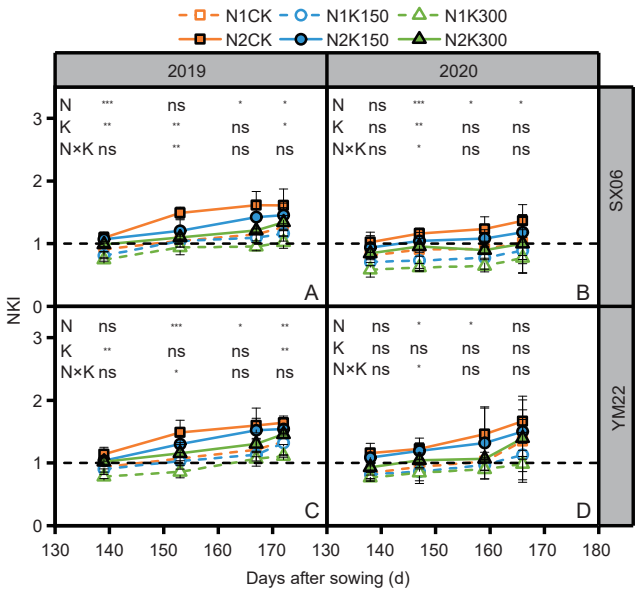


Fig. 8 Effects of N–K interactions on the N–K interaction index (NKI) of different wheat cultivars during the growing seasons in 2018–2019 (A) and (C) and 2019–2020 (B) and (D). The results in this figure are verification results of field test data from the 2018–2019 and 2019–2020 seasons. SX06 and YM22 represent Shengxuan 6 and Yangmai 22, respectively. N1 and N2 represent N application rates of 120 and 240 kg ha^{-1}, respectively. CK, K150 and K300 represent K application rates of 0,150 and 300 kg ha^{-1}, respectively. Bars mean SD (n=3). *, ** and *** indicate significant differences at the 10, 5 and 1% levels, respectively; ns indicates no significant difference.

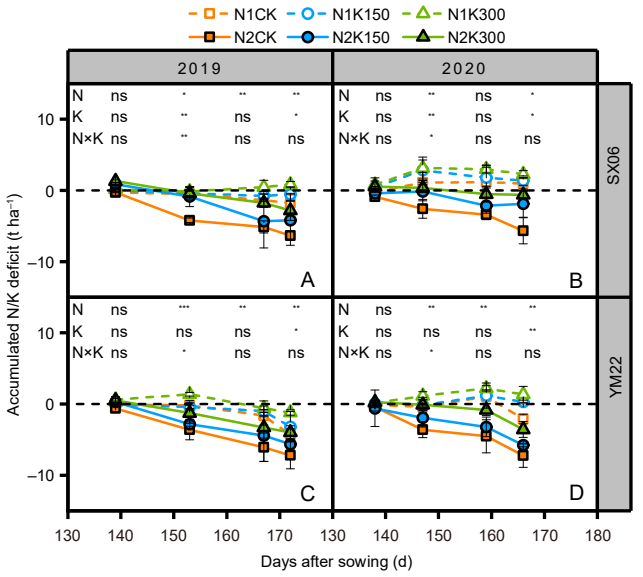


Fig. 9 Effects of N–K interactions on the accumulative nitrogen and potassium ratio deficit (N/K$_{ad}$) of different wheat cultivars in the growing seasons in 2018–2019 (A) and (C) and 2019–2020 (B) and (D). The results in this figure are verification results of field test data from the 2018–2019 and 2019–2020 seasons. SX06 and YM22 represent Shengxuan 6 and Yangmai 22, respectively. N1 and N2 represent N application rates of 120 and 240 kg ha^{-1}, respectively. CK, K150 and K300 represent K application rates of 0,150 and 300 kg ha^{-1}, respectively. Bars mean SD (n=3). *, ** and *** indicate significant differences at the 10, 5 and 1% levels, respectively; ns indicates no significant difference.

seasons and the collected literature data were used to analyze the quantitative relationships between the nutritional indices and relative yields (RYs) during different growth periods. The RY shows a linear plus plateau relationship with NNI and KNI, but it has a downward-opening quadratic relationship with NKI (Fig. 12). The three indices all showed excellent estimation performance at the heading stage, with R^2 values of 0.73, 0.74, and 0.86 for the fitting curves. The NKI performed best and explained 86% of the variation. All three indices exhibited poor fitting during the flowering stage; in particular, the KNI did not exhibit a significant relationship with RY during the anthesis stage. When the optimal yield was achieved, the corresponding NNI values ranged from 0.840 to 0.867, the KNI ranged from 0.896 to 0.964, and the NKI ranged from 0.813 to 1.014. Generally, compared with NNI and KNI, the prediction accuracy of NKI for RY was improved by 11.63 and 17.44%, respectively, under N–K interactions.

4. Discussion

4.1. Comparative analysis of critical K concentration dilution curves

The critical nutrient dilution curve is a crop nutrient management method based on the allometric relationship between aboveground biomass accumulation and nutrient absorption (Gómez *et al.* 2019; Lemaire *et al.* 2019; Adiele *et al.* 2021). Like that of N, the dilution effect of the crop K concentration was more obvious in the early growth stage and gradually stabilized with crop growth, which was consistent with the results of previous studies (Salette and Huche 1991; Greenwood and Stone 1998; Gallardo *et al.* 2021). This variation may stem from the fact that metabolic tissue biomass, which is crucial for crop growth, forms a smaller portion of plant biomass compared to the structural tissue biomass, which tends to have lower K concentrations (Lemaire *et al.* 2019; Adiele *et al.* 2021; Cheng *et al.* 2022). In this study, we effectively developed a generalized CKDC for wheat plants grown under different N planting strategies using the Bayesian method proposed by Makowski *et al.* (2020), which, when combined with CNDC, provides insights into the assessment of wheat N and K status in East China (Fig. 3). Our results revealed significant differences in CKDC and parameter A1 across different N levels. However, the disparity between the globally fitted curve and the curve fitted at each N level was minor and failed to achieve statistical significance (Fig. 4). Fontana *et al.* (2022) analyzed biomass and K concentration data from wheat plants collected during vegetative growth in a long-term experiment of more than 30 years and hypothesized that N deficiency may have an impact on CKDC; however, the extent to which N deficiency causes this impact requires further study. In this study, compared with the N1 treatment, the soil N supply was greater in the N2 treatment, resulting in the dominant N–K synergistic absorption effect in the plants, which led to changes in K availability, thus affecting the growth and development of

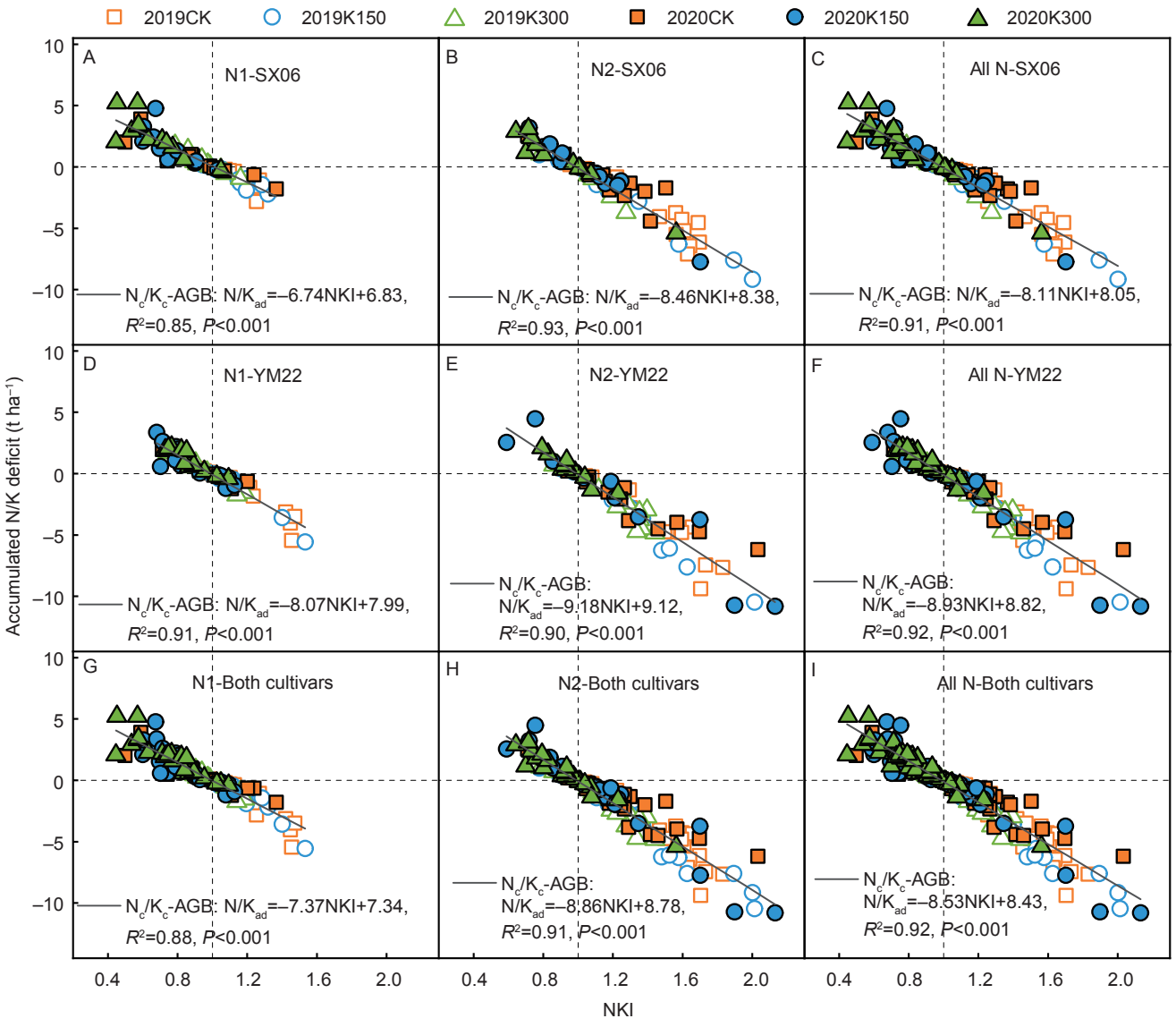


Fig. 10 Relationships between N–K interaction index (NKI) and the accumulative nitrogen and potassium ratio deficit (N/K$_{ad}$) calculated based on the critical nitrogen to potassium concentration ratio dilution curve based on the aboveground biomass (N$_c$/K$_c$-AGB) curve model under the N–K interactions of different cultivars. The results in this figure are verification results of field test data from the 2018–2019 and 2019–2020 seasons. SX06 and YM22 represent Shengxuan 6 and Yangmai 22, respectively. N1 and N2 represent N application rates of 120 and 240 kg ha^{-1}, respectively. CK, K150 and K300 represent K application rates of 0,150 and 300 kg ha^{-1}, respectively.

the wheat plants. However, although high N improved the CKDC, no notable disparities were evident among the CKDCs established across various cultivars. Considering the limited data on the establishment of CKDCs and the uncertainty of related parameters, statistically small differences between different N levels and cultivars are acceptable. In addition, studies have indicated that insufficient soil moisture also affects N availability in the soil, which in turn impacts the K uptake status of plants (Zhang *et al.* 2010; Coskun *et al.* 2017), leading to a greater underestimation of the K concentration under a low N supply. But in this study, there was no drought stress during the wheat growing seasons, so we cannot determine whether the KNI we constructed is applicable to soil water deficit conditions. In addition, our experimental field did not suffer from N deficiency, so we are unsure if the KNI can be used under N-limited conditions. However, we found that the difference between the KNI values calculated with the generalized CKDC and those calculated with the specific CKDC under different N levels was not significant, at least at N levels of 120–240 kg ha^{-1}. To some extent, this proved that the change in K concentration caused by N deficiency can be ignored, but further research is needed to verify this conclusion.

In this study, compared with N1 (K_c=2.90AGB$^{-0.29}$), parameter A1 was greater in N2 (K_c=3.89AGB$^{-0.35}$), which showed that the application of N fertilizer promoted the absorption and utilization of K by plants and was conducive to dry matter accumulation under the same K application conditions. There was no significant difference between parameter A2 at the N1 and N2 levels, indicating that when

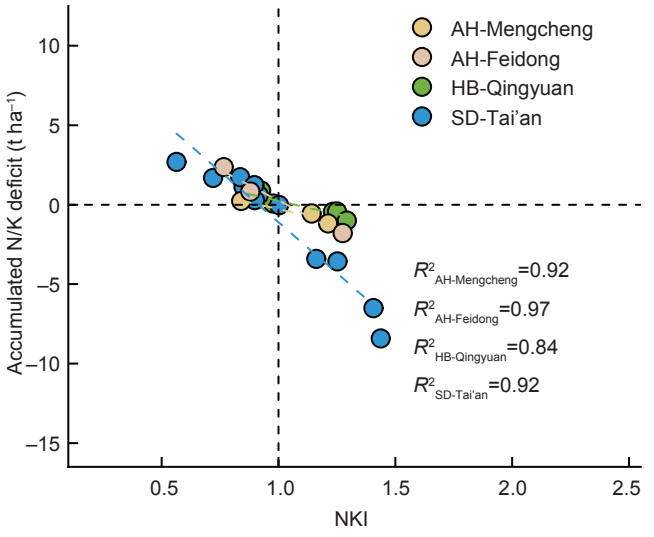


Fig. 11 Relationships between the N–K interaction index (NKI) and the accumulative nitrogen and potassium ratio deficit (N/K$_{ad}$) calculated based on the critical nitrogen to potassium concentration ratio dilution curve based on the aboveground biomass (N$_c$/K$_c$-AGB) in the major wheat-growing provinces in China. The colors of the points represent the four sites in three major wheat-growing provinces, where AH, HB and SD represent Anhui, Hebei and Shandong provinces, China, respectively.

N fertilizer was applied within this range under the same K fertilization conditions, the K concentration of the plant increased and slowly decreased to the same extent as the biomass increased. In addition, there was a significant difference in the A1 value between the CKDC constructed by Fontana *et al.* (2022) and the generalized CKDC constructed in this study. This may be due to the K-rich soil and salts in Switzerland, as well as varying soil types and water availability across the regions, all of which can influence K mineralization rates and microbial activity. However, parameter A2 (dilution rate of PKC) was not affected, possibly because this parameter is a statistical parameter that is only slightly affected by climatic factors (Zhao 2014; Cheng *et al.* 2022). In contrast, the A1 value is relatively more susceptible to ecological conditions and technological treatments (Yao *et al.* 2021). The relative uncertainty of the parameters decreased when incorporating all the data across all cropping modes and years, which is consistent with the findings of Soratto *et al.* (2022). When a sufficiently large dataset is used, the formulated CKDC is more robust, minimizing the uncertainties stemming from inadequate experimental design, sampling, and errors in analysis and calculations. Therefore, this study has certain reliability in constructing a generalized CKDC under a certain range of N levels.

4.2. Effects of N–K interactions on the N and K nutritional status of wheat

The nutritional balance of N and K is usually affected by the application of N or K fertilizers (Grzebisz *et al.* 2020), and maintaining a balanced N and K status is the key to optimizing wheat quality and yield. In general, calculating the changes in NNI and KNI during the growth period through critical N and K dilution curves can intuitively determine the N and K status (Lemaire *et al.* 2019; Adiele *et al.* 2021). Regardless of the level of N application, the application of more K fertilizer increased the NNI and KNI (Figs. 6 and 7). However, Ning *et al.* (2013) demonstrated that increasing K application did not enhance the yield under low N conditions. With high N levels, K application reduces the NNI, mitigates excessive growth, promotes balanced biomass distribution in tender branches, nourishes roots, and ultimately enhances yield. Conversely, high N and low K can increase the NNI, leading to robust development of aboveground components and an imbalance between N and K (Zhao *et al.* 2017). Therefore, when conducting fertilizer management for wheat, the interactions between plant N and K should be analyzed simultaneously, as these interactions play important roles in N and K management.

A single-element nutritional diagnosis is insufficient for managing crop growth, and the combined application of N and K fertilizers can significantly increase yields (Zhao *et al.* 2017). Excess N leads to vigorous growth of aboveground stems and leaves, resulting in yield reduction (Deng *et al.* 2023). Adequate K nutrition facilitates the transport of photosynthetic products from the ground to the ear, enhancing the dry matter distribution ratio in the ear. Figs. 6 and 7 reveal that at the booting stage, the interaction between N and K significantly influenced NNI but did not have a significant effect on KNI. Furthermore, Fig. 8 demonstrates that NKI exhibited significant N–K interaction effects during the booting stage. These results confirm that N plays a dominant role in the effects of N and K co-limitation on plant N and K status. In addition, in the present study, under a low N level in the early growth period, the NNI values were lower than 1 for the various K treatments. This phenomenon could be attributed to the increased demand for K during early stem elongation, which leads to the inhibition of N absorption by the plant. Early N deficiency may not adversely impact yield, while late N deficiency, such as that occurring around the anthesis stage for most food crop varieties, can have a substantial impact on yield by affecting both grain number and weight (Rodriguez *et al.* 2024). For instance, initial and temporary N deficiency in wheat (NNI<1 before stem elongation) might not have an impact on yield if adequate N nutrition is reinstated before anthesis (NNI=1) (Ravier *et al.* 2017). Our findings corroborate those observations, as the KNI value under a high N level and the NNI value under a low N level both approach 1 as the growth period progresses, particularly during the heading stage (Figs. 6 and 7). This suggests a collaborative interaction between N and K during early plant growth and development, ensuring the nutritional requirements for grain formation in later developmental stages. In addition, N improves K uptake by plants and increases dry matter weight. Hence, by regulating N to affect plant absorption of K, changing the ratio between N and K can maintain high biomass, and biomass under high N conditions is more relevant to grain yield (Rodriguez *et al.* 2024).

4.3. Comparison of the responses of different nutritional indicators to wheat yield

NNI and KNI are also considered key indicators for assessing

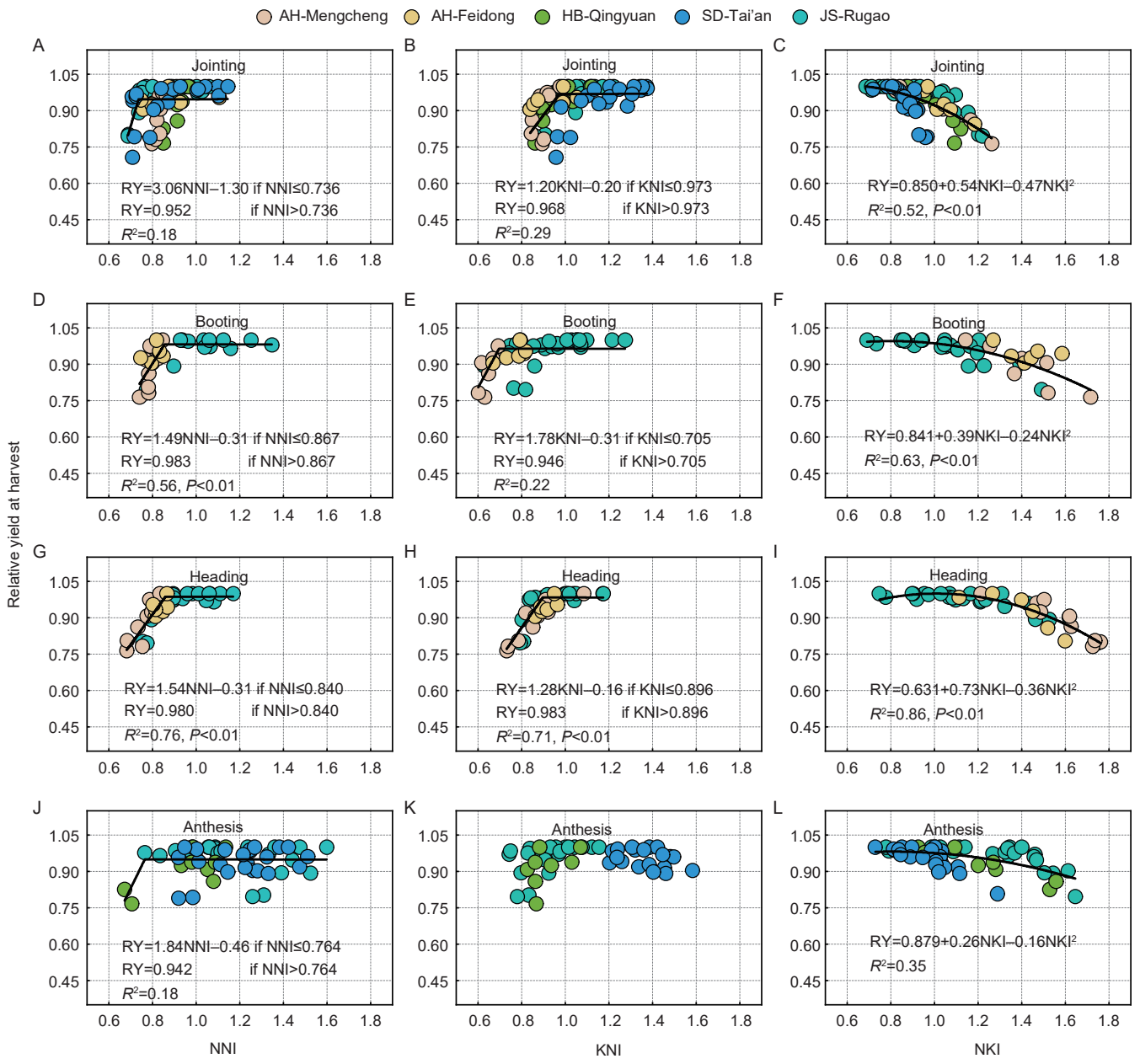


Fig. 12 Relationships between the nutritional indices and relative yield (RY) in the main growth periods of major winter wheat production provinces in China. The colors of the points represent different sites in the four provinces, where AH, HB, SD, and JS represent Anhui, Hebei, Shandong, and Jiangsu provinces, respectively. NNI, N nutrition index; KNI, K nutrition index; NKI, N–K interaction index.

crop yield and are widely used for evaluating the yields of various crops (Lemaire *et al.* 2019; Adiele *et al.* 2021; Cheng *et al.* 2022; Li W *et al.* 2024). In this study, we compared the relationships between three nutrient indicators (NIs) (NNI, KNI, and NKI) and RY, and the results showed that they were all strongly correlated during the heading stage, with NKI having the highest R^2 value (Fig. 12). A recent report re-examined the relationship between NNI and yield (Rodriguez *et al.* 2024), and the results also confirmed that the best predictability occurred around the anthesis period (Justes *et al.* 1997). Notably, NNI and KNI exhibited linear+plateau relationships with RY, while NKI and RY exhibited a quadratic parabolic relationship with a downward opening, which is similar to the results of previous studies (Gómez *et al.* 2019; Cheng *et al.* 2022; Deng *et al.* 2023). The results demonstrated the reliability of NI-based plant nutritional status and yield assessments (Gómez *et al.* 2019; Lemaire *et al.* 2019; Adiele *et al.* 2021). In addition, the RY exhibited stability after the critical thresholds for both NNI and KNI were reached, where the maximum yield was achieved with a critical threshold of approximately 1 (Zhao *et al.* 2014). In this study, we found the NNI threshold at which the optimal RY occurred was 0.840 to 0.867, that for KNI ranged from 0.896 to 0.964, and that for NKI ranged from 0.813 to 1.014 (Fig. 12). However, as the NKI reaches the maximum yield when it is close to 1, the yield will decrease as the NKI

continues to increase, which shows that excess N will lead to N and K imbalances and reduce yields.

Compared with NNI and KNI, NKI includes information on both N and K and is more comprehensive than a single element index. However, NKI cannot replace NNI or KNI for diagnosing the status of a single element (Kunrath *et al.* 2020) because it requires the simultaneous determination of N and K concentrations, which poses challenges with the current technology for field crops. However, using remote sensing to non-destructively estimate N and K concentrations, as well as aboveground biomass, provides a feasible method for calculating NKI (Deng *et al.* 2023; Li D *et al.* 2024). Therefore, NKI remains a significant covariate for interpreting data from genotype-environment interaction experiments amidst varying N and K conditions. So this variable can be used in precision nutrient management to understand the coupling of soil-to-plant N and K fluxes.

5. Conclusion

Previous studies on nutrient dilution curves often overlooked N–K interactions, whereas this study provides new insights into such interactions in wheat. In this study, Bayesian methods rooted in critical dilution curve theory were used to analyze the relationship between PKC and AGB in wheat crops subjected to various N and K treatments, in addition to assessing the uncertainties in parameters A1 and A2 for CKDC establishment. Specifically, increasing the application of N fertilizer increased A1, but had little effect on A2. Furthermore, NNI and KNI can quantify the indirect effects of N or K deficiency on crops, while the direct impact can be assessed through NKI, which is calculated by integrating CNDC and CKDC. The changes in crop growth in response to proportional changes in N and K concentrations could be determined by NKI. In addition, topdressing N fertilizer at the jointing stage significantly improved the N–K interaction effect on NNI and NKI at the booting stage, but it had no significant interaction effect on KNI. All indicators demonstrated the best predictive ability for RY at the heading stage, and compared with NNI and KNI, the prediction accuracy of NKI was improved by 11.63 and 17.44%, respectively. However, NKI still needs to be verified in more environments, such as those affected by drought, haze, frost and extreme temperatures.

Acknowledgements

This work was supported by the Jiangsu Independent Innovation Fund Project of Agricultural Science and Technology, China (CX(21)1006) and the Major Independent Innovation Program of Jiangsu Key Laboratory of Information Agriculture, China.

Declaration of competing interest

The authors declare that they have no conflict of interest.

Declaration of generative AI and AI-assisted technologies in the writing process

The authors declare that they did not use AI in the preparation and writing of this manuscript.

References

Adiele J G, Schut A G, Ezui K S, Pypers P, Giller K E. 2021. Dynamics of NPK demand and uptake in cassava. *Agronomy for Sustainable Development*, **41**, 1–14.

Adiele J G, Schut A G T, Ezui K S, Giller K E. 2022. LINTUL-Cassava-NPK: A simulation model for nutrient-limited cassava growth. *Field Crops Research*, **281**, 108488.

Alfoldi Z, Pinter L, Feil B. 1994. Nitrogen, phosphorus and potassium concentrations in developing maize grains. *Journal of Agronomy and Crop Science*, **172**, 200–206.

Bates T E. 1971. Factors affecting critical nutrient concentrations in plants and their evaluation: A review. *Soil Science*, **112**, 116–130.

Beaufils E R, Sumner M E. 1976. Application of the DRIS approach for calibrating soil, plant yield and plant quality factors of sugarcane. In: *Proceedings of the South Africa Sugar Technology Association*. Durban, South Africa. pp. 118–124.

Bélanger G, Ziadi N, Lajeunesse J, Jouany C, Virkajarvi P, Sinaj S, Nyiraneza J. 2017. Shoot growth and phosphorus–nitrogen relationship of grassland swards in response to mineral phosphorus fertilization. *Field Crops Research*, **204**, 31–41.

Cheng M, He J, Wang H, Fan J, Xiang Y, Liu X, Liao Z, Tang Z, Abdelghany A E, Zhang F. 2022. Establishing critical nitrogen dilution curves based on leaf area index and aboveground biomass for greenhouse cherry tomato: A bayesian analysis. *European Journal of Agronomy*, **141**, 126615.

Ciampitti I A, Fernandez J, Tamagno S, Zhao B, Lemaire G, Makowski D. 2021. Does the critical N dilution curve for maize crop vary across genotype×environment×management scenarios? — A Bayesian analysis. *European Journal of Agronomy*, **123**, 126202.

Coskun D, Britto D T, Kronzucker H J. 2017. The nitrogen–potassium intersection: Membranes, metabolism, and mechanism. *Plant, Cell & Environment*, **40**, 2029–2041.

Deng L, Xu X, Zhu Y, He W, Jin M, Liu Y, Lu G, Lv Z. 2023. Changes in dilution curves of critical nitrogen concentration in sweetpotato under different potassium conditions. *Field Crops Research*, **303**, 109130.

Fontana M, Hirte J, Bélanger G, Makowski D, Elfouki S, Sinaj S. 2022. Long-term K fertilization effects on soil available K, grain yield, and plant K critical value in winter wheat. *Nutrient Cycling in Agroecosystems*, **123**, 63–82.

Gallardo M, Cuartero J, de la Torre L A, Padilla F M, Segura M L, Thompson R B. 2021. Modelling nitrogen, phosphorus, potassium, calcium and magnesium uptake, and uptake concentration, of greenhouse tomato with the VegSyst model. *Scientia Horticulturae*, **279**, 109862.

Gómez M I, Magnitskiy S, Rodríguez L E. 2019. Critical dilution curves for nitrogen, phosphorus, and potassium in potato group Andigenum. *Agronomy Journal*, **111**, 419–427.

Greenwood D J, Karpinets T V, Zhang K, Bosh-Serra A, Boldrini A, Karawulova L. 2008. A unifying concept for the dependence of whole-crop N:P ratio on biomass: Theory and experiment. *Annals of Botany*, **102**, 967–977.

Greenwood D J, Stone D A. 1998. Prediction and measurement of the decline in the critical-K, the maximum-K and total cation plant concentrations during the growth of field vegetable crops. *Annals of Botany*, **82**, 871–881.

Grzebisz W, Szczepaniak W, Bocianowski J. 2020. Potassium fertilization as a driver of sustainable management of nitrogen in potato (*Solanum tuberosum* L.). *Field Crops Research*, **254**, 107824.

He P, Yang L, Xu X, Zhao S, Chen F, Li S, Tu S, Jin J, Johnston A M. 2015. Temporal and spatial variation of soil available potassium in China (1990–2012). *Field Crops Research*, **173**, 49–56.

Hou W, Yan J, Jákli B, Lu J, Ren T, Cong R, Li X. 2018. Synergistic effects of nitrogen and potassium on quantitative limitations to photosynthesis in rice (*Oryza sativa* L.). *Journal of Agricultural and Food Chemistry*, **66**, 5125–5132.

Huang S, Miao Y, Cao Q, Yao Y, Zhao G, Yu W F, J Shen J, Yu K, Bareth G. 2018. A new critical nitrogen dilution curve for rice nitrogen status diagnosis in Northeast China. *Pedosphere*, **28**, 814–822.

Jarvis S C, Macduff J H, Webb J, Mosquera A. 1990. Effects of nitrate supply and deprivation and/or defoliation on potassium absorption and distribution in ryegrass. *Journal of Experimental Botany*, **41**,

1–10.
Justes E, Mary B, Meynard J M, Machet J M, Thelier-Huché L. 1994. Determination of a critical nitrogen dilution curve for winter wheat crops. *Annals of Botany*, **74**, 397–407.
Justes E, Jeuffroy M H, Mary B. 1997. Wheat, barley, and durum wheat. In: Lemaire G, ed., *Diagnosis of the Nitrogen Status in Crops*. Springer, Berlin, Heidelberg. pp. 73–91.
Kunrath T R, Lemaire G, Teixeira E, Brown H E, Ciampitti I A, Sadras V O. 2020. Allometric relationships between nitrogen uptake and transpiration to untangle interactions between nitrogen supply and drought in maize and sorghum. *European Journal of Agronomy*, **120**, 126145.
Lemaire G. 2012. *Diagnosis of the Nitrogen Status in Crops*. Springer Science & Business Media, Germany.
Lemaire G, Jeuffroy M H, Gastal F. 2008. Diagnosis tool for plant and crop N status in vegetative stage: Theory and practices for crop N management. *European Journal of Agronomy*, **28**, 614–624.
Lemaire G, Sinclair T, Sadras V, Bélanger G. 2019. Allometric approach to crop nutrition and implications for crop diagnosis and phenotyping. A review. *Agronomy for Sustainable Development*, **39**, 1–17.
Li D, Yang S, Du Z, Xu X, Zhang P, Yu K, Zhang J, Shu M. 2024. Application of unmanned aerial vehicle optical remote sensing in crop nitrogen diagnosis: A systematic literature review. *Computers and Electronics in Agriculture*, **227**, 109565.
Li J, Zhou Y, Gu H, Lu Z, Cong R, Li X, Ren T, Lu J. 2023. Synergistic effect of nitrogen and potassium on seed yield and nitrogen use efficiency in winter oilseed rape (*Brassica napus* L.). *European Journal of Agronomy*, **148**, 126875.
Li W, Gu X, Fang H, Zhao T, Yin R, Cheng Z, Tan C, Zhou Z, Du Y. 2024. Optimizing nitrogen application rate by establishing a unified critical nitrogen dilution curve for maize under different mulching planting patterns. *European Journal of Agronomy*, **152**, 127026.
Lollato R P, Figueiredo B M, Dhillon J S, Arnall D B, Raun W R. 2019. Wheat grain yield and grain-nitrogen relationships as affected by N, P, and K fertilization: A synthesis of long-term experiments. *Field Crops Research*, **236**, 42–57.
Makowski D, Zhao B, Ata-Ul-Karim S T, Lemaire G. 2020. Analyzing uncertainty in critical nitrogen dilution curves. *European Journal of Agronomy*, **118**, 126076.
Mondal S D M. 1982. Potassium nutrition at high levels of nitrogen fertilization on rice. *Potash Review*, **3**, 1–4.
Ning Y W, Ma H B, Xu X J, Wang J D, Zhang H, Xu J P, Chen J, Zhang Y C. 2013. Effects of deficiency of N, P, or K on growth traits and nutrient uptakes of sweetpotato at early growing stage. *Scientia Agricultura Sinica*, **46**, 486–495. (in Chinese)
Parent L E, Dafir M. 1992. A theoretical concept of compositional nutrient diagnosis. *Journal of the American Society for Horticultural Science*, **117**, 239–242.
Plummer M. 2017. JAGS Version 4.3.0 User Manual. Lyon, France.
Ravier C, Meynard J M, Cohan J P, Gate P, Jeuffroy M H. 2017. Early nitrogen deficiencies favor high yield, grain protein content and N use efficiency in wheat. *European Journal of Agronomy*, **89**, 16–24.
Rodriguez I M, Lacasa J, van Versendaal E, Lemaire G, Belanger G, Jégo G, Sandaña P G, Soratto R P, Djalovic I, Ata-Ul-Karim S T, Reussi Calvo N I, Giletto C M, Zhao B, Ciampitti I A. 2024. Revisiting the relationship between nitrogen nutrition index and yield across major species. *European Journal of Agronomy*, **154**, 127079.
Sadras V O. 2005. A quantitative top-down view of interactions between stresses: Theory and analysis of nitrogen–water co-limitation in Mediterranean agro-ecosystems. *Australian Journal of Agricultural Research*, **56**, 1151–1157.
Salette J, Huche L. 1991. Diagnosis of the mineral nutrition status of a pasture through herbage analysis: Principles, implementation, examples. *Fourrages*, **125**, 3–18. (in French)
Sattari S Z, van Ittersum M K, Bouwman A F, Smit A L, Janssen B H. 2014. Crop yield response to soil fertility and N, P, K inputs in different environments: Testing and improving the QUEFTS model. *Field Crops Research*, **157**, 35–46.
Soratto R P, Sandaña P, Fernandes F M, Fernandes A M, Makowski D, Ciampitti I A. 2022. Establishing a critical nitrogen dilution curve for estimating nitrogen nutrition index of potato crop in tropical environments. *Field Crops Research*, **286**, 108605.
Vizcayno-Soto G, Côté B. 2004. Boundary-line approach to determine standards of nutrition for mature trees from spatial variation of growth and foliar nutrient concentrations in natural environments. *Communications in Soil Science and Plant Analysis*, **35**, 2965–2985.
Williams R D. 1957. Growth and nutrition of timothy (*Phleum pratense* L.) iii. absorption and distribution of nitrogen, phosphorus and potassium during the first year of growth. *Annals of Applied Biology*, **45**, 664–673.
Xie K, Lu Z, Pan Y, Gao L, Hu P, Wang M, Guo S. 2020. Leaf photosynthesis is mediated by the coordination of nitrogen and potassium: The importance of anatomical-determined mesophyll conductance to CO_2 and carboxylation capacity. *Plant Science*, **290**, 110267.
Yan S, Wu Y, Fan J, Zhang F, Zheng J, Qiang S, Guo J, Xiang Y, Zou H, Wu L. 2020. Dynamic change and accumulation of grain macronutrient (N, P and K) concentrations in winter wheat under different drip fertigation regimes. *Field Crops Research*, **250**, 107767.
Yao B, Wang X, Lemaire G, Makowski D, Cao Q, Liu X, Liu L, Liu B, Zhu Y, Cao W. 2021. Uncertainty analysis of critical nitrogen dilution curves for wheat. *European Journal of Agronomy*, **128**, 126315.
Zhang F, Niu J, Zhang W, Chen X, Li C, Yuan L, Xie J. 2010. Potassium nutrition of crops under varied regimes of nitrogen supply. *Plant and Soil*, **335**, 21–34.
Zhao B. 2014. Determining of a critical dilution curve for plant nitrogen concentration in winter barley. *Field Crops Research*, **160**, 64–72.
Zhao B, Yao X, Tian Y, Liu X, Ata-Ul-Karim S T, Ni J, Cao W, Zhu Y. 2014. New critical nitrogen curve based on leaf area index for winter wheat. *Agronomy Journal*, **106**, 379–389.
Zhao Q X, Jiang Y, Shi C Y, Si C C, Shi X J, Wang W Q, Liu H J, Shi Y X. 2017. Effect of nitrogen–potassium interaction on absorption and translocation of nitrogen and potassium in sweetpotato and the root yield. *Plant Physiology Journal*, **53**, 889–895.
Ziadi N, Brassard M, Bélanger G, Claessens A, Tremblay N, Cambouris A N, Nolin M C, Parent L É. 2008. Chlorophyll measurements and nitrogen nutrition index for the evaluation of corn nitrogen status. *Agronomy Journal*, **100**, 1264–1273.

Executive Editor-in-Chief Shaokun Li
Managing Editor Ning Wang